A SPECTRUM-INDEPENDENT PROCEDURE FOR CORRECTING EDDY FLUXES MEASURED WITH SEPARATED SENSORS

JOHANNES LAUBACH[1] and KEITH G. McNAUGHTON[2]
[1]*Horticulture and Food Research Institute of New Zealand, P.O. Box 23, Kerikeri 0470, New Zealand E-mail: jlaubach@hort.cri.nz;* [2]*Paretu Drive, R.D1, Kerikeri 0470, New Zealand*

(Received in final form 2 July 1998)

Abstract. We investigate flux underestimates in eddy correlation measurements that are caused by horizontal separation of the sensors. A common eddy correlation setup consists of a sonic anemometer and a humidity sensor which, because of its bulk, must be placed some distance away from the sonic path, leading to a flux loss (of latent heat). Utilizing an additional fast temperature sensor placed near the humidity sensor, we develop a procedure for correcting for this loss. The procedure simultaneously corrects the sensible heat flux for the difference between true temperature and sonic temperature. Our correction procedure, which does not depend on the shape of the cospectrum, is then compared to the widely-used procedure following Moore (1986), which assumes a cospectral model ('Kansas Model'). Both correction methods are applied to data collected within the internal boundary layer over a rice paddy, downwind of arid land. Under conditions of good fetch, they were found to agree well. Under poor fetch conditions, the model-based correction tended to be too small, while the spectrum-independent combined correction was robust. The latter is thus recommended for situations where the cospectral shape can be expected to deviate from the 'Kansas' shape.

Keywords: Advection, Cospectral model, Eddy correlation, Sensor separation, Surface fluxes.

1. Introduction

Eddy correlation is a popular technique for measuring the turbulent fluxes of mass and energy in the atmospheric boundary layer. It relies on the basic definition of a flux: the flux density of a scalar variable is velocity times the concentration of the scalar. In a turbulent flow field, both these factors fluctuate over several decades of frequency, but only fluctuations that are mutually correlated contribute to the flux. In order to determine accurate temporal averages of the flux, both factors have to be measured fast enough to capture these correlated fluctuations. However measurement systems invariably suffer, to some degree, from technical restrictions decorrelating the time series of the two factors. One such restriction is the distance between sensors. The effect of this sensor separation will be investigated in this paper, and a new, simple, and robust method to correct for it will be proposed.

The ideal experimental system for eddy correlation will measure all variables directly, accurately and at the same point, using small sensors with fast frequency response and optimized in shape to avoid flow distortion. Of course, real eddy correlation systems fail to meet this ideal. Measuring turbulent fluctuations directly

Boundary-Layer Meteorology **89:** 445–467, 1998.

is always subject to limitations by frequency-response characteristics of the measurement system. For example, the combination of a sonic anemometer and an open-path gas analyzer has the following response limitations: the sonic averages wind and temperature fluctuations over a finite acoustic path length (miniaturization is restricted by the need for robustness), the gas analyzer measures absorption of a finite volume of air (size reduction would decrease the signal-to-noise ratio), and because the gas analyzer is relatively bulky and will distort the flow around it, it has to be placed some distance away from the sonic anemometer. Each of these three features involves geometrical dimensions of order of a few decimeters. They restrict the ability of the system to resolve turbulent structures that are not large compared to them, and thus act as low-pass filters. Further high-frequency losses can occur due to operating characteristics of the instruments, for instance electronic filters, or the rotational speed of a chopper wheel in the gas analyzer.

Mathematically, the flux losses are described best in the frequency domain. There, a scalar flux is obtained by integrating the cospectrum of wind velocity and the scalar over frequency. Each physical effect causing a flux loss can be represented by a frequency-dependent transfer function. The product of all transfer functions equals the ratio of the measured to the unknown true cospectrum. Moore (1986) discussed several transfer functions comprehensively: those for sensor response, electronic filtering, digital sampling, line-averaging of the sensor path (or, more generally, volume-averaging), and separation of two sensors whose data are to be correlated. Others were added later, dealing with different effects when bringing air samples to a closed-path sensor via an intake tube (recently reviewed by Leuning and Judd, 1996), or for treatment of mismatching response times (recently reassessed by Horst, 1997).

Three-dimensional sonic anemometers are now the preferred choice to measure velocity fluctuations. Since these instruments also provide a temperature measurement, sensible heat fluxes are obtained easily, and without separation losses. To measure other scalar fluxes, additional sensors are needed. Two of the scalars most sought after are water vapour and carbon dioxide, for they are important variables in surface energy budgets and plant processes. One option for measuring both simultaneously is using an infrared gas analyzer (IRGA). The combination of sonic and IRGA is increasingly being used above various ecosystems that are often complex or patchy both in their roughness and energy partitioning characteristics (e.g., Fan et al., 1990, 1992; Neumann et al., 1994; Wofsy et al., 1993).

Such a combination of a sonic anemometer and an open-path IRGA was used in the experiment that is reported below. With this instrumentation, the separation effect will typically be the most important term to reduce measured fluxes. Separation losses are hard to avoid because any bulky sensor close to the sonic would distort the flow to be measured, thus a minimum distance must be kept, although it is not easily quantified. Flux losses due to the sensors' path lengths (or averaging volumes) may or may not be significant. In our case they are not, as will be shown in the first part of the 'Results' section. For this reason, we focus on

sensor separation, which means that in practice we approximate the total transfer function by the separation transfer function.

Lee and Black (1994) did not use spectral transfer functions when they investigated how the separation flux loss depends on stability and orientation of the separation path relative to the wind. Instead, their derivation is based on structure functions. For large separation distances, this approach predicts the resulting flux loss much more accurately than the approach using the spectral transfer function from Moore (1986); for small distances, the results of the two methods converge. We do not follow Lee and Black (1994) for two reasons: firstly, because the separation of our sensors was small enough to permit Moore's simpler approach, and secondly, because Lee and Black restricted their treatment to unstable stratification over homogeneous terrain, while our experiment deals with a stable internal boundary layer.

The approach using spectral transfer functions has some practical disadvantages: one either has to calculate the shape of the cospectrum for each averaging period by means of a Fourier transform, or assume a shape *a priori*, then apply the correction, and finally integrate the corrected cospectrum to obtain the desired flux. The former procedure consumes a lot of computing time and may sometimes fail altogether due to noisy sensors or aliasing. The alternative of assuming a spectral model is computationally simpler and thus often preferred. In most cases the assumed cospectrum is the 'Kansas cospectrum' (Kaimal et al., 1972).

The Kansas Model (henceforth used without quotation marks) describes the spectral behaviour over ideal homogeneous terrain, meaning that the turbulent fluxes are fully equilibrated to the underlying surface conditions and obey Monin-Obukhov similarity. Its validity for non-ideal terrain, however, is expected to be limited. In this paper we deal with a situation of hot, dry air being advected over a heavily transpiring crop. This is a situation where Monin-Obukhov similarity cannot be assumed *a priori*. This prompted us to explore a spectrum-independent procedure for flux correction.

Our procedure employs a thermocouple placed close to the humidity sensor (an open-path IRGA), to obtain a temperature signal not only from the sonic, but at the location of the IRGA as well. In principle, having fast temperature measurements at both locations allows a straightforward separation correction. However things are a little more complicated because the sonic measures acoustic virtual temperature instead of temperature, and in the advective inversion the difference is considerable. Because of that, we combine the temperature and humidity data at the location of the IRGA to obtain acoustic virtual temperature there. An empirical correction factor is then calculated from the ratio of the acoustic virtual temperatures at the IRGA's location and the sonic's location. The correction factor can then be applied individually to the fluxes of sensible heat, latent heat, and any other scalar measured at the IRGA's location. The correction procedure does not assume any particular cospectral shapes, and is suitable for on-line processing. The fact that it combines a separation correction with a correction from acoustic virtual temperature flux to

true temperature flux is a nice new aspect, but only a side issue. The main purpose of this paper is to investigate whether the proposed technique for determining the flux loss directly is reliable and preferable to the correction method using a spectral model.

2. Theory

2.1. Separation flux loss and spectral correction

Let $w(t)$ be a time series of vertical wind and $a(t)$ a time series of a scalar variable, e.g., temperature or humidity. The vertical turbulent flux of a over a finite averaging period is then given by the covariance $\overline{w'a'}$ (overbars denoting temporal means, and primes denoting deviations from the mean). This covariance can be spectrally decomposed as

$$\overline{w'a'} = \int_0^\infty C^{wa}(f)\,\mathrm{d}f, \tag{1a}$$

where $C^{wa}(f)$ stands for the true cospectrum of w and a, and f is frequency. Equation (1a) refers to an ideal measurement, with w and a obtained at the same point in space and time. However if the scalar sensor is separated from the wind sensor by a distance s, which we indicate by using s as a subscript, then the cospectrum will be subject to some high-frequency loss, and the observed covariance will be somewhat different:

$$\overline{w'a'_s} = \int_0^\infty C_s^{wa}(f)\,\mathrm{d}f. \tag{1b}$$

The flux loss due to sensor separation can be expressed by the ratio of the covariances with and without separation. We call this ratio the 'covariance reduction factor' γ:

$$\gamma = \overline{w'a'_s}/\overline{w'a'}. \tag{2a}$$

Strictly speaking, γ should bear a superscript 'wa' also, but this has been dropped because we assume identical spectral shapes for different scalars. This is true whenever they are highly correlated or anticorrelated, and it is a much weaker requirement than Monin-Obukhov similarity (because cospectral similarity only requires the scalar fluxes to have similar spatial distributions, while Monin-Obukhov similarity requires horizontal homogeneity of the surface fluxes).

The observed and the true cospectrum are related by the transfer function for separation, G_s:

$$G_s(f) = C_s^{wa}(f)/C^{wa}(f). \tag{2b}$$

G_s depends on the separation distance s and on properties of the turbulent flow. Moore (1986) gave the following expression for it, which is an empirical fit based on the derivations of Irwin (1979) and Kristensen and Jensen (1979):

$$G_s(f) = \exp\left[-9.9\left(\frac{fs}{u}\right)^{1.5}\right], \tag{3}$$

where u is the mean horizontal wind. This formula is designed for lateral separation, but according to Moore (1986) it also describes the longitudinal case well, provided that s is small. Note that for a given instrumental setup u is the only time-dependent parameter in Equation (3).

With $G_s(f)$ known, the covariance reduction factor can be obtained directly by inserting Equations (1a) and (2b) into Equation (2a):

$$\gamma = \overline{w'a'_s} \Big/ \int_0^\infty C_s^{wa}(f)/G_s(f)\,\mathrm{d}f. \tag{4}$$

However it requires a lot of computational time to apply a Fourier transform and a subsequent integration for every single run of data. This procedure is also error-prone when the high-frequency part has a low signal-to-noise ratio, or is subject to aliasing.

A simpler and quicker correction procedure can be used when the form of the cospectrum is known *a priori*. This is the case in an equilibrium surface layer where Monin-Obukhov similarity is satisfied so that cospectra for all scalars follow the same 'Kansas' form (Kaimal et al., 1972). We denote the Kansas model cospectrum by C_K^{wa}, and insert this together with Equations (1b) and (2b) into Equation (2a) to obtain

$$\gamma = \int_0^\infty C_K^{wa}(f)G_s(f)\,\mathrm{d}f \Big/ \int_0^\infty C_K^{wa}(f)\,\mathrm{d}f. \tag{5}$$

This equation avoids the need to calculate the Fourier transform for each measurement run.

The Kansas cospectrum depends on the stability parameter $(z-d)/L$, where z is measurement height, d zero plane displacement, and L the Obukhov length, the latter defined by

$$L = -\frac{u_*^3\overline{T}}{kg\overline{w'T'_v}}, \tag{6}$$

with u_* friction velocity, k the von-Kármán constant, g gravity acceleration, T temperature, and T_v virtual temperature.

The original expression for $C_K^{wa}(f)$ (Kaimal et al., 1972) was modified by Moore (1986) to ensure normalization to unity in numerical computations. For

stable stratification, $(z-d)/L > 0$, it then reads (Moore's Equation (21a) with coefficients inserted):

$$fC_K^{wa}(f) = \frac{n}{0.284\Xi^{0.75} + 9.345\Xi^{-0.825}n^{2.1}}, \tag{7a}$$

where $n = f(z-d)/u$, and $\Xi = 1 + 6.4(z-d)/L$. In the unstable case, $(z-d)/L < 0$, Moore's Equation (25) gives:

$$fC_K^{wa}(f) = \begin{cases} \dfrac{12.92n}{(1+26.7n)^{1.375}} & \text{if } n < 0.54 \\ \dfrac{4.378n}{(1+3.8n)^{2.4}} & \text{if } n \geq 0.54. \end{cases} \tag{7b}$$

Thus, the cospectrum $C_K^{wa}(f)$ is determined by two flow parameters, namely u and $(z-d)/L$. Remembering that $G_s(f)$ according to Equation (3) depends only on u, it follows that insertion of Equations (3) and (7) into Equation (5) relates γ to u and $(z-d)/L$. The integrals in this relation can be evaluated numerically, or by analytic approximation. This can be done on-line as part of the flux calculation procedure, as demonstrated by Moore (1986). While this approach is highly practical, its accuracy relies on the validity of the cospectral model in the given experimental situation. We will develop a model-independent procedure in the next section.

2.2. Spectrum-independent correction procedure using an additional sensor

In some cases the cospectrum does not follow the Kansas shape. One option then is to determine the covariance reduction factor experimentally. This requires two identical sensors, made small enough to avoid significant flow distortion, placed at either end of the separation path. Fast thermocouples are a suitable choice. Let one of them be close to the w sensor, giving a temperature signal T, and the other close to the a_s sensor, giving a temperature signal T_s. By definition (Equation (2a)) the reduction factor γ equals the ratio of the w-T_s covariance to the w-T covariance. This same value of γ can be applied to the eddy flux of any other scalar, $\overline{w'a'_s}$, to retrieve its unknown counterpart $\overline{w'a'}$, provided that the spectral behaviour of a is similar to that of T.

We turn now to the instrumentation used in our experiment. There, the scalars of interest are humidity, measured by an open-path IRGA, and temperature. The w sensor is a 3-dimensional sonic anemometer that provides already a temperature measurement at zero separation distance. The setup considered above can thus be simplified by removing the fast temperature sensor close to the sonic anemometer. However the sonic measures the acoustic virtual temperature T_{av} instead of T (Schotanus et al., 1983, Kaimal and Gaynor, 1991). The two are related by

$$T_{av} = T(1 + 0.51q), \tag{8a}$$

where q is specific humidity. With Reynolds averaging and first-order approximation, it follows for the temperature fluctuations

$$T'_{av} = T' + 0.51\overline{T}q'. \tag{8b}$$

The two other terms of the expansion, containing $\overline{q}T'$ and $\overline{q'T'}$, are smaller and have been dropped. Note that the T_{av} signal from the sonic is assumed to be already corrected for the cross-wind error. For this reason the cross-wind term given by Schotanus et al. (1983) does not appear in Equation (8b).

Acoustic virtual temperature is just another scalar variable, as suitable as temperature, to determine the covariance reduction factor γ by means of Equation (2a). While T'_{av} is measured directly by the sonic anemometer, $T'_{av,s}$ is obtained from Equation (8b) using the data of the humidity sensor and the temperature sensor next to it. Thus

$$\gamma = \frac{\overline{w'T'_s}}{\overline{w'T'_{av}}} + 0.51\overline{T}\frac{\overline{w'q'_s}}{\overline{w'T'_{av}}}. \tag{9}$$

Dividing the raw temperature flux obtained from the displaced sensor by γ gives the corrected temperature flux, and doing the same with the raw humidity flux gives the corrected humidity flux. If the difference between T and T_{av} is negligible, then Equation (9) collapses to Equation (2a), and $\overline{w'T'}$ is obtained directly from the sonic anemometer. Because Equation 9 combines the separation flux loss correction and the humidity correction of the sonic temperature, we refer to it in the following as the 'combined correction'.

Equation (9) is sufficient to carry out the correction. How it works in detail can be understood by decomposing it spectrally. The spectral coefficients of acoustic temperature flux are linearly composed of the cospectra of temperature flux and humidity flux:

$$C^{wT_{av}}(f) = C^{wT}(f) + 0.51\overline{T}C^{wq}(f). \tag{10}$$

This is an implication of the same first-order approximation that leads from Equation (8a) to Equation (8b). We can now insert Equation (10) into Equation (2b), which is the definition of G_s, for the special case $a = T_{av}$. Doing so not for the 'true' cospectrum C^{wa}, but instead for the measured C_s^{wa} is possible provided that the measurement of T does not affect that of q, and vice versa. It results in:

$$G_s(f) = \frac{C_s^{wT}(f)}{C^{wT_{av}}(f)} + 0.51\overline{T}\frac{C_s^{wq}(f)}{C^{wT_{av}}(f)}. \tag{11}$$

This is the desired spectral decomposition. It describes the transfer function that is implicitly assumed when applying Equation (9) to correct fluxes. Calculating Equation (11) explicitly for a given dataset provides a means to compare the combined correction to spectral correction methods that rely on Equation (3).

3. Site and Experimental Details

The experiment ran from January 19 to February 9, 1997, over a flood-irrigated rice field at Warrawidgee, near Griffith, NSW, Australia (34°15′ S, 145°45′ E). To the west of the field, sparsely vegetated dry land extended for hundreds of kilometers. The site was selected to represent the special case of an advective inversion. Typically, we found air temperatures near 305 K from noon to sunset, and a flux Bowen ratio $H/\lambda E = -0.2$, where

$$H = \rho c_p \overline{w'T'}, \tag{12}$$

is the sensible heat flux, ρ being density and c_p specific heat at constant pressure of air, and

$$\lambda E = \rho \lambda \overline{w'q'}, \tag{13}$$

the latent heat flux, λ being latent heat of vaporization of water. The given numbers result in $\overline{w'T'_{av}}/\overline{w'T'} = 0.68$, which clearly shows that we cannot neglect the difference between acoustic temperature and true temperature.

Two identical eddy correlation systems were set up on the same tower, at 2.58 m and 4.47 m height, respectively, above firm ground. On the ground there was a layer of 0.03 m loose material (soil and organic) and above that a water layer of 0.17 m. The height of the rice crop increased from 0.77 m on 21 Jan to 0.86 m on 5 Feb, relative to firm ground, and its canopy density also increased during the experiment. First subtracting the layers below water level, and then removing the zero plane displacement, estimated as two-thirds of canopy height (Oke, 1987), left effective measurement heights ($z - d$) of 2.0 and 3.9 m, respectively.

The field was of rectangular shape, orientated almost north-south (deviation −4°). The tower was set up close to the eastern border to maximize fetch and acceptance angle for westerly winds because they represented the desired conditions of a well-developed stable internal boundary layer (IBL). Distances measured from the tower to the field borders were: 418 m to the west, 307 m to the north, 23 m to the east, and 271 m to the south. For winds from NW to SW this resulted in fetch-to-height ratios from 100:1 to 150 : 1 at the upper level and twice these values at the lower level. While the adjacent land to the west was almost ideally homogeneous (flat and dry), in the other directions lay a patchwork of similar-sized fields of the Murrumbidgee Irrigation Area, with a mixture of rice, wheat, stubble and burnt stubble. The field adjacent to the east was burnt off shortly before the experiment, so that easterly winds (unfortunately not infrequent) provided us with a contrasting dataset of 'worst-possible' fetch conditions in terms of energy fluxes. With easterly winds, locally stable conditions at the lower and unstable conditions at the upper level were observed, but neither represented a layer adjusted to either the rice paddy or the dry stubble.

Each eddy correlation system consisted of a 3-dimensional sonic anemometer, Model CSAT-3 (Campbell Scientific, Logan, Utah), an open-path infra-red gas analyzer (IRGA) for water vapour and carbon dioxide similar to the one described by Auble and Meyers (1992), and a fast-response chromel-constantan thermocouple (Type E) of diameter 12.7 μm (1/2000″), provided by Campbell Scientific as an optional add-on to the CSAT-3. The sonic probes were facing west and the IRGAs mounted at about 0.3 m separation distance south-east of the sonic paths. Instead of placing the thermocouple next to the sonic path, a metal wedge was inserted where its supporting bar is supposed to be attached to the CSAT-3 probe, fixing the bar at an oblique angle and placing the thermocouple close to the IRGA path. In practice, the distance from thermocouple to sonic path was 5 cm less than that from IRGA to sonic path. According to the manufacturer, the CSAT-3 corrects for the cross-wind error of acoustic virtual temperature fluctuations internally (E. Swiatek, 1996, pers. comm.). This justifies the use of Equation (8b) for the relation between T' and T'_{av}.

Measurements were taken during daylight hours. Eddy correlation data were sampled at 10 Hz and averaged over 20 min. A higher sampling rate than 10 Hz had been planned, but could not be realized. Unfortunately, this caused some aliasing problems at windspeeds over 5 m s^{-1}. Additional sensors were operated, at a sampling rate of 1 Hz, to determine the available energy A defined as

$$A = R_n - G - \Delta Q_w, \tag{14}$$

where R_n is net radiation, G soil heat flux, and ΔQ_w the heat storage change in the water layer. These sensors were a net radiometer CN-1 (Middleton Instruments, Melbourne, Australia), two soil heat flux plates placed under the loose material on the firm ground, one beneath a dense part of the rice canopy, the other beneath a less dense part, and two water temperature sensors at the same locations. The latter were each made of a series of thermocouple junctions in a 215 mm long non-transparent plastic tube. This was fixed to the ground by a nail and stood almost vertically in the water by means of its own buoyancy. These devices provided depth-integrated averages of the water temperature.

On January 31 the IRGA at the upper level was removed for calibration. We used this period to assess the covariance reduction due to sensor separation directly. This was done by placing both available thermocouples at this height, one adjacent to the sonic path, the other in its usual position 0.25 m away from it. Wind direction on this day was E to SE, representing the ‘worst-possible’ fetch conditions as described above.

4. Results and Discussion

4.1. Magnitude of the flux corrections

Let us begin by evaluating the importance of the proposed corrections. To calculate the expected covariance reduction factor γ for our setup we apply Equation (5), inserting the transfer functions for separation (Equation (3)) and path-averaging according to Moore (1986), and using the Kansas cospectrum from Equation (7a). The resulting γ depends on measurement height and on two variable parameters: windspeed u and stability parameter $(z-d)/L$. In Figure 1, γ is shown at the lower height, $z-d$ = 2.0 m, as a function of u and for $(z-d)/L$ = 0.05, which is a stability value close to the median of all 'good fetch' periods collected at Warrawidgee. It can be seen that γ is typically 0.85 to 0.90, equivalent to flux losses $(1-\gamma)$ of order 10 to 15%. The losses are smaller at the upper height (not shown) because the cospectrum is shifted to lower frequencies there; they increase with increasing stability, because the cospectrum is shifted to higher frequencies. Figure 1 also shows that flux losses due to path-averaging are small compared to the effect of sensor separation. This justifies our focus on the separation correction.

Theoretically, our 'combined correction' (Equation (9)) should produce similar results. Before we investigate how well that holds in practice, we give an example how relevant the combined correction is in absolute terms. This is displayed in Figure 2, for a sunny day with a stable IBL. There, both the corrected and uncorrected H and λE are shown as well as the residue of the energy budget

$$R = A - H - \lambda E, \tag{15}$$

with and without flux corrections. H is typically changed by 20–50 W m^{-2}, while λE corrections can be as high as 200 W m^{-2}, which is a considerable fraction of the available energy. Note that the second term in Equation (9) forms a significant part of the combined correction, as can be seen by comparing the raw H_{av} from the sonic, which is free of separation errors, to the corrected H. The residue R calculated from uncorrected fluxes is systematically biased to positive values. The correction reduces R, in some cases by up to 150 W m^{-2}, as a consequence of the changes in H and λE. Thus, much of the systematic bias is removed by the correction, while the scatter of R does not change in a noticeable way. We have a closer look at this finding further below. So far, Figure 2 shows that the flux changes resulting from application of Equation (9) amount to a considerable fraction of the available energy, and that the changes tend to improve closure of the energy budget.

4.2. Direct assessment of separation loss corrections

As described in the Theory section, the covariance reduction due to sensor separation can be assessed directly with two temperature sensors. We did this for a few hours on January 31, at our upper measurement level. Correlated with the

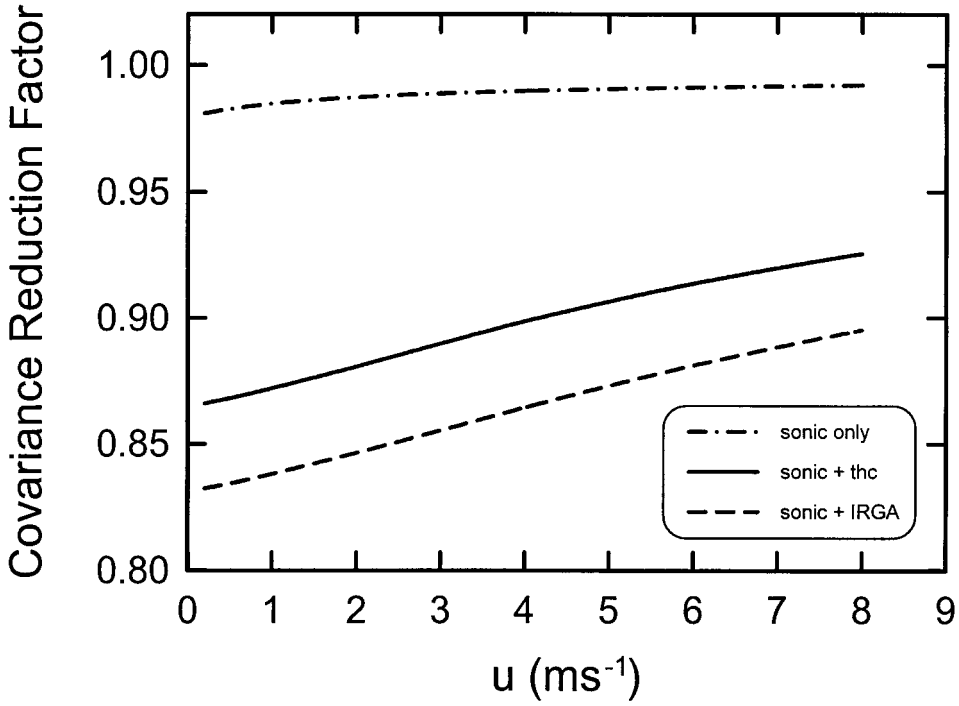

Figure 1. Covariance reduction factors for scalar fluxes from the instruments mounted at $z - d$ = 2.0 m, calculated with the transfer functions for separation and path averaging following Moore (1986), and assuming the Kansas cospectrum (Equation (7a)) for stability $(z - d)/L$ = 0.05. The dash-dotted line represents the path averaging on both temperature and vertical velocity measurements by the sonic anemometer. The solid line combines the sonic's path averaging for vertical wind with the effect of separation of a point sensor for temperature 0.25 m away. The dashed line represents the net effect of sonic path averaging, scalar (IRGA) path averaging and separation (0.30 m) on the humidity flux.

vertical wind data from the sonic, the thermocouple data provide the separation transfer function G_s empirically (Equation (2b)). In addition, these data provide a test of the robustness of the model-based cospectral correction procedure, for they represent poor fetch conditions. Wind direction on this day was E to SE, so that the dry-to-wet transition lay only 37 m upwind of the instruments. This resulted in locally slightly unstable conditions at $z - d$ = 3.9 m. Because of the poor fetch the spectral shape is expected to deviate from the ideal, equilibrated shape of the Kansas Model.

Using the Kansas Model (inserting Equation (7b) into Equation (5)), we obtain an almost constant value of γ = 0.95 during this period. γ hardly varies because variations of horizontal wind u are small (between 1.2 and 2.7 m s^{-1}) and because in unstable cases the cospectrum does not depend on the stability parameter. As opposed to this, γ values from the direct comparison of the thermocouples (Equation (2a)) vary over the range 0.60–0.95. To understand this, we turn our attention

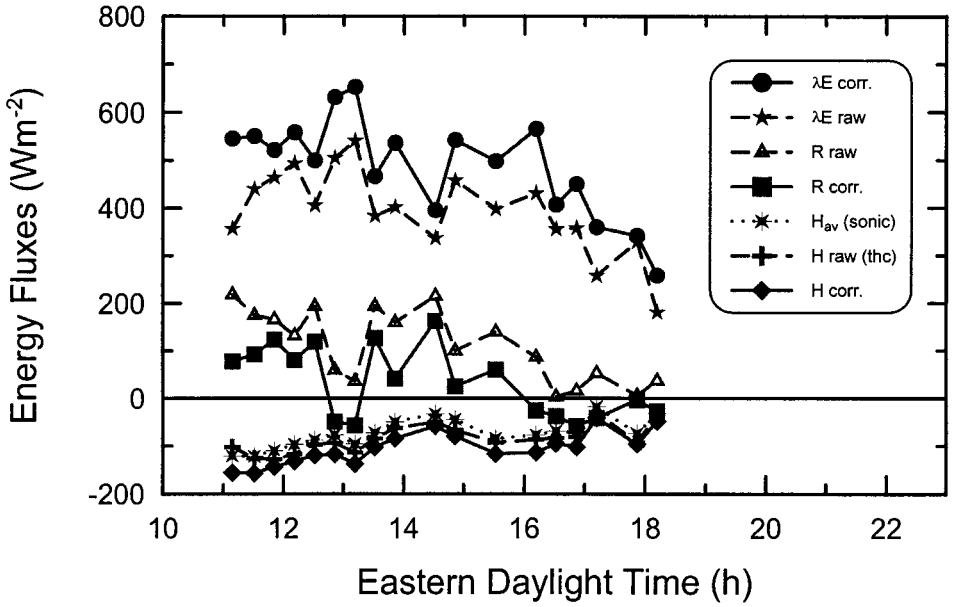

Figure 2. Sensible heat fluxes, latent heat fluxes, and resulting residues of the energy budget with and without correction according to Equation (9) on February 5 at $z - d$ = 2.0 m.

to the spectral behaviour of the heat fluxes and their corrections. Figure 3 provides an example that represents fair agreement of the two γ estimates: measured 0.88, modelled 0.96. Figure 3a shows that the shapes of the w-T cospectra obtained with the close and the displaced thermocouple agree excellently in all their major structures for frequencies below 1 Hz. At higher frequencies there are discrepancies, as expected. They are more obvious on Figure 3b, where the ratio of the distant to the nearby thermocouple is displayed. The ratio scatters around 1 at low frequencies and drops off at higher frequencies. This ratio is the separation transfer function G_s, as determined empirically by Equation (2b). Also plotted is G_s according to Equation (3) (Moore, 1986). Dismissing the scatter, the two independent estimates of G_s agree well, which means that G_s as predicted from Moore (1986) describes the flux loss accurately.

Because the agreement of the transfer functions is so good, there must be another reason why, sometimes, large differences in the resulting covariance reduction factors occur. The only other possible source of these is the cospectral shape itself. To demonstrate this, we look again at Figure 3a, where the modelled (Kansas) cospectral shape is plotted as well as the two measured. (The modelled cospectrum is normalized to the same total covariance.) There is no frequency range in which the measured and modelled cospectrum agree quantitatively. Instead, in the measured cospectrum, deep excursions in the mid- and low-frequency ranges tend to decrease the overall contributions of these ranges to the total covariance, hence the high-frequency end has stronger relative weight than it has in the modelled

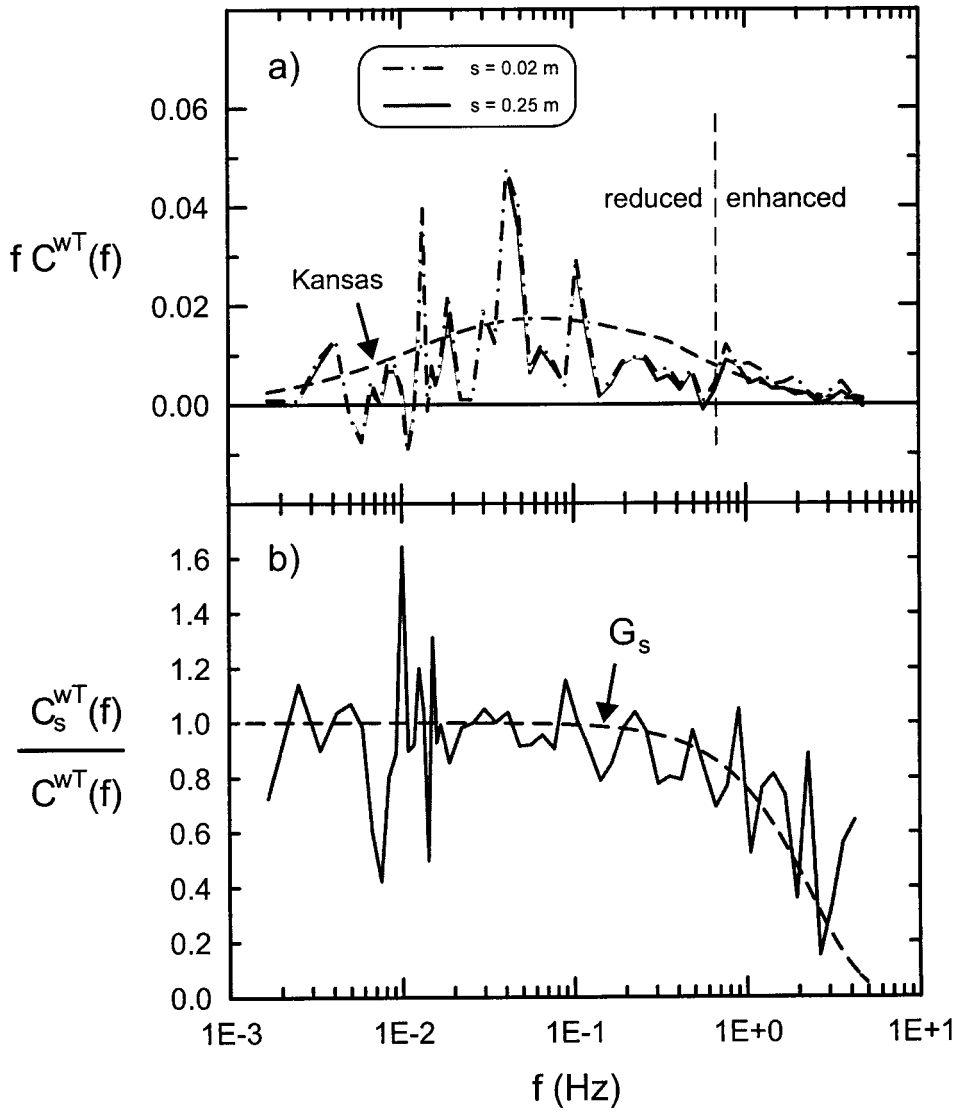

Figure 3. (a) Cospectrum of sensible heat flux for the period 15 : 01–15 : 21 h on 31 Jan 97 as measured with a thermocouple near the sonic anemometer and a thermocouple at 0.25 m horizontal separation distance. Also shown is the ideal Kansas cospectrum (Equation (7b)). Mean horizontal wind: 2.52 m s^{-1}, mean wind direction: 137°. (b) Cospectral ratio of heat flux from the sonic anemometer with distant thermocouple to the heat flux obtained from the sonic with close thermocouple. The dashed line represents the separation transfer function G_s from Equation (3).

cospectrum. Since the covariance reductions described by G_s affect only the higher frequencies, the true overall value of γ is lower than the model prediction of 0.96.

It might be argued that because of the poor fetch conditions the fluxes are not meaningful at all. However this is not the important point here. The point is that if the true cospectral shape deviates significantly from the modelled, then the model-based procedure fails to predict γ accurately. In this case empirical methods are preferable. One option would then be to apply the calculation-intensive procedure of Equation (4) with the measured cospectrum and G_s (from Moore or empirically determined). Alternatively, Equation (9) can be used, which is done in the next section.

4.3. Comparison of separation loss corrections in stable conditions

For the bulk of data from the Warrawidgee experiment, there are no direct measurements of the covariance reduction factor available, because there was no temperature sensor mounted next to the sonic anemometer. Being short of a genuine 'reference', we will assess the performance of the combined correction (Equation (9)) in three ways: first, by comparing to the Kansas Model, second, by investigating the spectral composition of the transfer function according to Equation (11), and third, by demonstrating its effect on the energy budget closure.

The dataset is restricted here to averaging periods with excellent fetch conditions, defined as those periods with wind from the western sector (180 to 360°) for at least 99% of the time. This criterion leaves a total of 70 runs at either height. With only 4 exceptions each, they all represent (slightly) stable conditions in the range $(z-d)/L$ = 0.0005 to 0.4, the medians being 0.062 at the upper and 0.050 at the lower height. (We determined L from the sonic anemometer data, using $\overline{w'T'_{av}}$ to approximate the buoyancy flux $\overline{w'T'_v}$ in Equation (6), and $(-\overline{u'w'})^{1/2}$ to estimate friction velocity u_*.) We reduced the dataset further by eliminating a few cases of high windspeed where we believe the data were affected by aliasing.

To compare the combined correction and the separation correction using the Kansas Model, the covariance reduction factors γ as obtained by both methods are shown in Figure 4, plotted against stability. The Kansas Model estimates form a narrow band between 0.93 and 0.89 for $(z-d)/L < 0.1$, and decrease rapidly for larger stability. The decrease is mainly due to the cospectrum shifting to higher frequencies, so being more strongly attenuated by the transfer function G_s. Three features can be noted in Figure 4: the scatter is larger for the empirical γ than for the modelled γ, the decrease of the empirical values with stability appears less pronounced, and the empirical γ are on average a few percent smaller than those modelled.

The magnitude of the scatter matches the expectations, given that each of the three measured covariances in Equation (9) is subject to a sampling error. Note that as $\overline{w'T'_{av}}$ approaches zero, Equation (9) becomes singular. Setting the left-hand

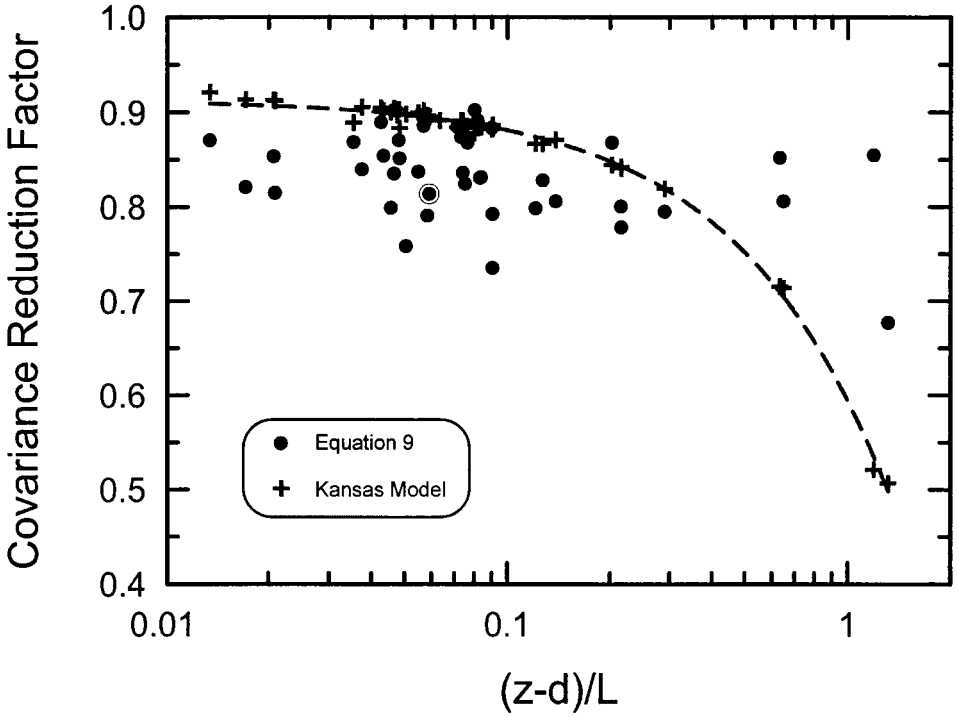

Figure 4. γ as calculated from Equation (9) and as obtained from Kansas Model versus stability $(z-d)/L$ at height $z-d$ = 2.0 m for all 20-minute-periods with wind direction from the Western sector at least 99% of the time. The same plot for $z-d$ = 3.9 m looks similar, but γ is usually closer to 1 (not shown). The circled dot indicates the interval selected for presentation of cospectra in Figure 5.

side to zero and solving for the ratio of sensible to latent heat flux gives a critical flux Bowen ratio, $H/\lambda E_{\text{crit}}$. This critical ratio is slightly temperature-dependent, but always close to -0.06. Compared to this, the data in Figure 4 represent Bowen ratios between -0.1 and -0.8, where Equation (9) is more robust, but still sensitive to small $\overline{w'T'_{av}}$. (As a practical guideline from our data, the magnitude of this term should not be less than 0.03 K m s^{-1}.)

The decrease of the empirical values of γ with stability is less pronounced than that of the modelled values, because we usually find the bulk of spectral energy located at lower frequencies than predicted by the Kansas Model (an example, which will be discussed below, is given in Figure 5a). This feature is found to be particularly strong for the few data points at $(z-d)/L > 0.2$. These runs have in common that horizontal wind u is below 1.8 m s^{-1}, and that the measured cospectrum peaks at approximately half a frequency decade lower than the modelled. In turn, the high-frequency end of the measured cospectrum has less relative weight than that of the model cospectrum, and consequently, separation losses were less than modelled.

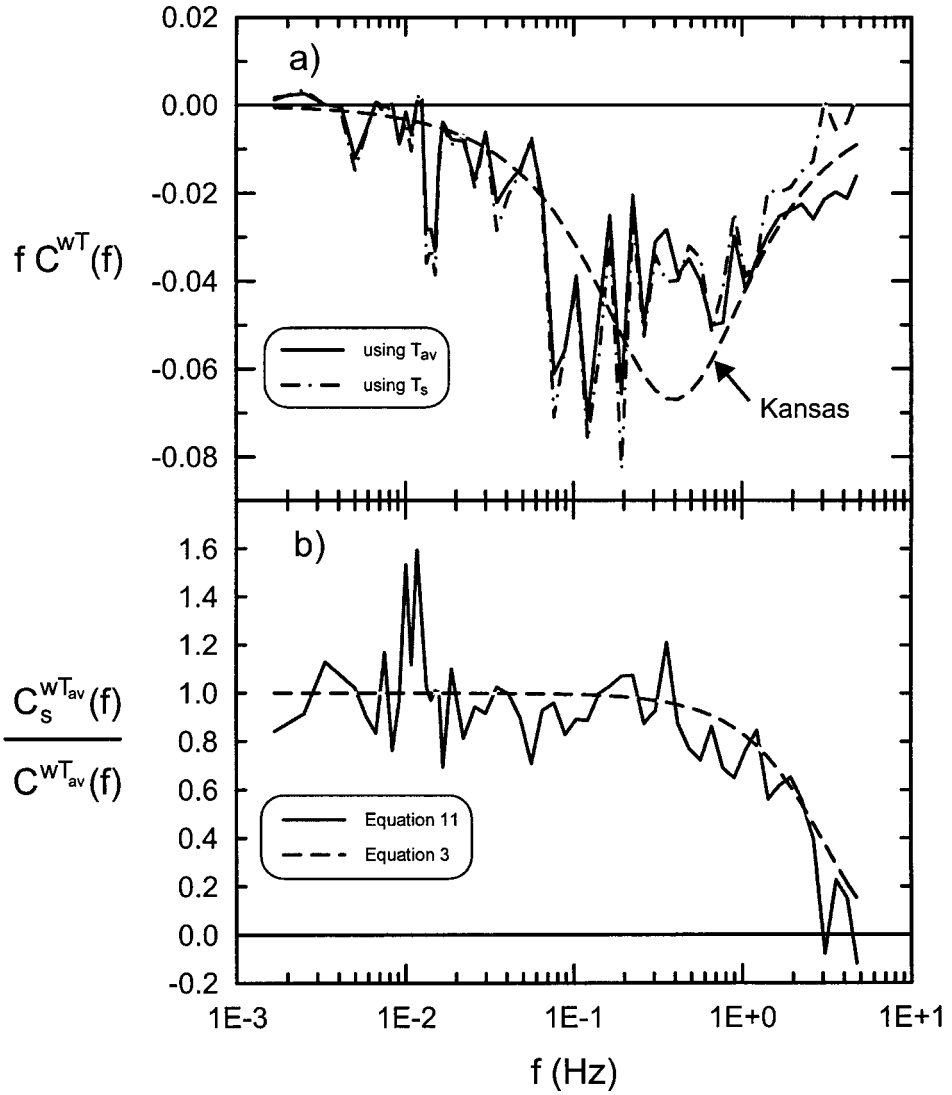

Figure 5. (a) Cospectra for the period 12 : 55–13 : 15 h on 8 Feb 97 at $z - d$ = 2.0 m: acoustic temperature flux from sonic anemometer (T_{av}) and temperature flux from sonic and thermocouple at 0.25 m horizontal separation distance (T_s). Also shown is the ideal Kansas cospectrum (Equation (7a)) normalized to the same area as for the T_{av} flux. Mean horizontal wind: 3.59 m s^{-1}, mean wind direction: 306°, stability: $(z - d)/L$ = 0.059. (b) Transfer function G_s from measured cospectral ratios using Equation (11), and modelled following Moore (1986), see Equation (3).

There remains the question why the calculated γ are, in general, smaller than the modelled. This is the same result as in the previous section, but for different conditions. For the data in the previous section, the fetch was ill-defined and the spectral shape far from the ideal Kansas shape. Here we consider a dataset with a fetch-to-height ratio of about 200 : 1 and thus might expect the Kansas Model to be a better approximation. To find out how well this expectation holds, and to investigate further, it is again necessary to look at the cospectra. A typical example of cospectra and transfer functions is given in Figure 5. In this run, the modelled γ is 0.895 and the calculated 0.81, about 10% less.

Looking first at the cospectral shapes (Figure 5a) it is found that indeed the Kansas Model provides a good match at high frequencies, where separation losses are relevant, and, with some scatter due to sampling uncertainties, at very low frequencies. The largest differences between modelled and measured cospectrum occur in a region around the peak, approximately from 0.05 to 1 Hz. The measured peak frequency is lower than modelled, and the scatter between neighbouring cospectral coefficients is very large. These features affect temperature fluxes and humidity fluxes (not shown) identically, and they are very common throughout our dataset. Cospectra with similar features were published by Lang et al. (1983) for a similar advective inversion. They seem to be characteristic of this situation. It is not necessary here to discuss the mechanism of the apparent peak shift further, because it occurs at frequencies that are almost unaffected by separation flux losses, except for the few cases of high stability. Figure 5a shows that, contrary to the case of poor fetch conditions, a distorted relative weighting of high and low frequencies cannot be the reason for mismatching γ.

Having stated this, we investigate the cospectral ratios according to Equation (11). The two terms there, describing the temperature and the humidity contributions, are of opposite signs because of the stable conditions. Only their sum is shown in Figure 5b, as a solid line. This is the transfer function representing the combined correction. In its overall shape, it agrees well with the theoretical transfer function (Equation (3)), which is drawn as a dashed line. Particularly in the cutoff region the agreement is convincing. However in the region between 0.4 and 0.8 Hz the empirical G_s is markedly below the modelled, and, to a lesser degree, also over almost two decades of even lower frequencies. To understand this, we remember that there is a slight conceptual difference between Figure 5b and the similar presentation in the previous section, Figure 3b. There, the empirical transfer function derives directly from two identical temperature sensors, and thus refers only to the separation effect, as it ideally should be. In Figure 5b, though, the empirical transfer function includes other properties of the instrumentation, because they can affect the three cospectral terms in Equation (11) to different degrees and do not necessarily cancel when forming the ratios. It is these properties that are likely to cause the mismatch between the two estimates of G_s, and thus the 10% difference in the estimates of γ.

We can rule out path averaging as the main cause, because its cutoff is effective at higher frequencies than that of the separation. Two other mechanisms are more likely candidates. The first is aliasing: if it is present, then sonic temperature will be most affected by it, because w' and T'_{av} at frequencies above the Nyquist frequency are still correlated, so will be folded back in the cospectrum and appear at lower frequencies. For separated sensors, however, the covariance that can be folded back will be largely reduced due to the low correlation at high frequencies. Consequently, forming both ratios on the right-hand side of Equation (9) with aliased covariances will tend to give smaller numbers than unaliased. In other words, the effect of aliasing on cospectra is that high-frequency flux *losses* will be folded back to lower frequencies. A numerical simulation revealed that this can indeed affect the cospectra over about two decades by a few percent. Thus, in addition to the direct effect described by Equation (3), sensor separation can potentially reduce the correlation of two variables indirectly, when combined with instrumental limitations.

The other possible mechanism is the uncertainty of optimum correlation due to the streamwise part of the sensor separation and due to the sampling time differences of the data acquisition system. In our setup, the sonic anemometer data were sent to the computer via a serial communication cable, while the IRGA and thermocouple data were sampled by a multichannel analog-to-digital acquisition board. Although our software routinely shifted the q_s and T_s data to achieve maximum correlation with the w data, there was always an uncertainty of one sampling interval, i.e., 0.1 s. As with aliasing, the effect of this uncertainty can amount to a few percent reduction in the cospectra and over one to two decades below the Nyquist frequency. Of course, the cospectrum of w and T_{av} is not subject to such a reduction.

Given that both effects are small and partly hidden in the general scatter, it is unrealistic to identify them in detail. But since they both work to reduce the covariance of separated sensors more than that of w and T_{av}, they may well explain the bias between modelled and calculated γ. This bias should, in theory, disappear if the modelled transfer function (Equation (3)) was combined with others accounting for aliasing and shift uncertainty. An intriguing interpretation is that our combined correction has, inadvertently, corrected for several effects that reduced the correlation of separated sensors, but of which we were unaware.

Finally, we consider the effect of the separation corrections, both following Moore (1986) and using Equation (9), on the closure of the energy budget. An example of a diurnal course has already been shown in Figure 2. In Table I, the average residues R of our good-fetch runs (same dataset as in Figure 4) are given, as calculated with corrected and uncorrected eddy fluxes. Before correction we find a bias to positive R (meaning that the available energy is larger than the sum of eddy fluxes) of a little under 60 W m^{-2} on average. Applying Equation (9) to H and λE reduces 2/3 of this bias at the lower height and 1/3 at the upper height. Using the spectral correction (Equation (3)) instead, the remaining residues are larger, which

TABLE I

Residue of the energy budget, R, in W m^{-2}, as calculated using eddy fluxes without separation correction, with spectral correction following Moore (1986), and with combined correction (Equation (9)). The given numbers are averages of 42 runs.

$z - d$ (m)	R (no corr.)	R (spectral corr.)	R (combined corr.)
2.0	59	34	18
3.9	56	45	34

means the spectral correction method is less efficient in closing the energy budget. However the absolute values of R should not be overinterpreted: given the usual uncertainty of a few percent for 20-minute-averaged eddy fluxes, and in our special case the uncertainty of the large ΔQ_w term (heat storage in the water layer), then it must be stated that the closure is reasonably good at both heights anyway.

Still, the combined correction has a clearly systematic effect, as illustrated in Figure 6, where R is displayed against γ, at the lower height. Diamonds represent R before and dots after the correction of sensible and latent heat fluxes (before correction meaning that the sonic temperature was used to calculate H). The corrective effect of γ brings R close to the zero line even for the extreme values of $\gamma < 0.8$. This is a strong argument for the robustness of the procedure in periods when other flux losses (due to aliasing or uncertainty of relative time lag) add to the separation effect, or when the Kansas Model is an inappropriate description of the cospectral shapes. Typical afternoon values, when available energy is highest, are as follows: a value of $\gamma = 0.9$, which is the order of magnitude predicted by the Kansas Model, reduces R by about 30 W m^{-2}, while a value of 0.8 roughly doubles the effect. The improved closure of the energy budget is an indirect confirmation of the quality of the combined correction.

4.4. General discussion

The main purpose of Subsections 4.1–4.3 was to demonstrate that Equation (9) provides a practical approach to correct for flux losses due to sensor separation. A side issue that has been touched a few times is that at the same time it provides an elegant means to correct from acoustic virtual temperature fluxes to true temperature fluxes – better than the conventional way of doing so, because the humidity flux needed for this correction is automatically separation-corrected simultaneously. It was this aspect that suggested the name ‘combined correction’.

The net effect of the correction depends on the two terms contributing to Equation (9). Our experiment represented stable conditions. Sensible heat fluxes are then downward, while latent heat fluxes are upward. The magnitudes of both are

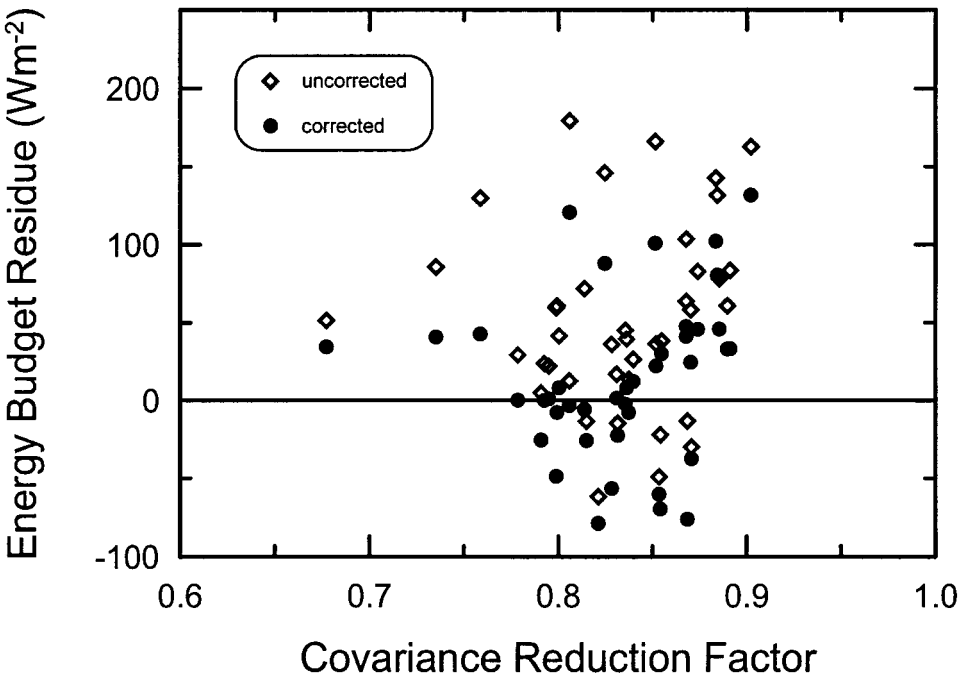

Figure 6. Energy budget residue R from uncorrected fluxes and after correction using Equation (9) at $z-d$ = 2.0 m. The mean R is 59 W m^{-2} for the uncorrected budgets and 18 W m^{-2} for the corrected (42 data points).

reduced by sensor separation. The uncorrected sensible heat flux (using T_{av} from the sonic anemometer) is also too small in magnitude because of the opposite sign of the humidity flux. Correcting the fluxes thus means to increase both upward λE and downward H, so that in the net energy budget their changes partly cancel. This explains why the shift between uncorrected and corrected R in Figure 6 is not larger, although Figure 2 displays fairly large changes especially for λE.

In unstable situations, the energy budget is composed differently. H and λE are then both upwards, competing for the available energy A. Consequently latent heat fluxes tend to be smaller, and the humidity term in Equation (9) is less important. Applying the correction then means that resulting sensible heat fluxes are smaller than those obtained from the sonic, while corrected latent heat fluxes are larger than the uncorrected, so that again the changes to R partly cancel.

The covariance reduction factor γ, as obtained from the combined correction method, is valid for scalar fluxes other than sensible and latent heat as well, as long as they fulfil the same requirements of cospectral similarity. To make use of this, the scalar under consideration must be measured at the same location as humidity (as is the case for CO_2 with our IRGAs), or at least at an identical distance s from the vertical wind measurement. This instrumentational requirement can be simplified if the humidity term in Equation (9) is small enough to be neglected, which

then results in Equation (2a). This variation of the empirical correction method is particularly attractive if a scalar, whose flux is of interest, cannot be measured close to either the wind sensor or the humidity sensor, or if no humidity sensor is available at all.

Kristensen et al. (1997) have proposed a different approach to deal with the separation of sensors. They concluded that mounting the scalar sensor underneath the wind sensor, instead of displacing it horizontally, retains correlation of vertical wind and the scalar much better, and thus reduces flux losses. It is undoubtedly a good idea to reduce losses, rather than to correct for them. Yet in some situations, such as within canopies, the value of this approach still has to be established. It might be worth considering to combine a vertically separated arrangement of sensors, following Kristensen et al. (1997), with our idea of using an additional temperature sensor to remove the remaining error. The value of this may be substantial since it appears that our empirical correction can compensate for some imperfections in the experimental system that are not directly due to, but are indirectly altered by separation of sensors.

Our method relies on similarity of the cospectra of temperature flux and humidity flux. This requirement was satisfied well in our experiment, except at very low frequencies where the contributions to the total fluxes were too small to be relevant. It can be imagined that temperature and humidity spectra might be less similar if their respective sensors were placed close to a field transition, or within a canopy where sensible and latent heat fluxes had different source areas. But these cases are usually linked with ill-defined fetch conditions, which implies that the spectral shapes can be very far from the ideal Kansas spectrum. In these cases, the spectral correction following Moore (1986) provides a poor alternative. While the model-based correction requires cospectral shapes of all scalar fluxes to be similar to the model cospectrum, the combined correction only requires similar shapes of C^{wT} and C^{wq}. The second requirement is easier to fulfil than the first.

5. Conclusions

The proposed ‘combined correction’ for sensible and latent heat fluxes has been demonstrated to remove flux errors due to sensor separation effectively. If the true cospectral shape is described well by the Kansas cospectrum, the combined correction must produce the same results as the generally accepted spectral method using the Kansas Model and transfer functions. It has been shown that, in practice, both methods agree well as long as the relative weight of the high-frequency part is similar for measured and modelled cospectra. In cases when the cospectral shapes do not follow the model cospectrum, the combined correction is the more reliable method because it is spectrum-independent. A second advantage of the combined correction is that it can remove all flux losses of separated sensors simultaneously, not only those due to the well-known effect of spatial decorrelation, but

also those due to some deficiencies of the data acquisition system, in as much as these deficiencies affect separated and non-separated sensors differently.

A limitation of the combined correction is a numerical instability when $\overline{w'T'_{av}}$ approaches zero. Because the denominator in Equation (9) is then very uncertain, the derived γ cannot be expected to be trustworthy. When sensible heat fluxes are small, it is better to correct latent heat fluxes and gas fluxes according to Moore (1986). A second limitation could occur if the spectral shapes of heat and water vapour flux were markedly different, because the two ratios in Equation (11) would be sensitive to that, but then the applicability of the spectral model would be limited too.

Having these limitations in mind, we conclude with a practical recommendation. Since the combined correction requires only one additional temperature sensor, and is thus not too costly, it should be seriously considered whenever the eddy correlation technique is used over non-ideal terrain and when significant separation distances of sensors cannot be avoided. It can be applied on-line as easily as the model-based spectral correction. The combined correction can also be used with the error-minimizing sensor positions advocated by Kristensen et al. (1997), because it is by no means restricted to horizontal sensor separation. In situations where cospectral shapes are not well-known, e.g., in canopies, the combined correction could even serve to assess if there, too, vertical sensor separation is preferable to horizontal separation.

Acknowledgements

The work was funded entirely by the Government of New Zealand (Marsden Fund Contract CO6539). Nonetheless, Australia's contribution to its success is significant due to the kind support we received from a number of its residents. We thank Angelo Silvestro for allowing us to work on his ideally-located rice paddy, the colleagues of CSIRO Land and Water at Canberra (Pye Laboratory) for providing tower, power and cover (caravan), the staff of CSIRO Land and Water at Griffith for local assistance and accomodation, and last not least Peter Isaac for providing good, quick and cheap calibrations of the IRGAs. One of the IRGAs is property of Flinders University (Adelaide), Institute for Meteorology and Atmospheric Science, and the other of NIWA (Gracefield, NZ). Their generosity in lending them to us is gratefully acknowledged.

References

Auble, D. L. and Meyers, T. P.: 1992, 'An Open Path, Fast Response Infrared Absorption Gas Analyzer for H_2O and CO_2', *Boundary-Layer Meteorol.* **59**, 243–256.

Fan, S.-M., Wofsy, S. C., Bakwin, P. S., Jacob, D. J., Anderson, S. M., Kebabian, P. L., McManus, J. B., Kolb, C. E., and Fitzjarrald, D. R.: 1992, 'Micrometeorological Measurements of CH_4

and CO_2 Exchange between the Atmosphere and Subarctic Tundra', *J. Geophys. Res.* **97**(D15), 16,627–16,643.

Fan, S.-M., Wofsy, S. C., Bakwin, P. S., Jacob, D. J., and Fitzjarrald, D. R.: 1990, 'Atmosphere-Biosphere Exchange of CO_2 and O_3 in the Central Amazon Forest', *J. Geophys. Res.* **95**(D10), 16,851–16,864.

Horst, T. W.: 1997, 'A Simple Formula for Attenuation of Eddy Fluxes Measured with First-Order-Response Scalar Sensors', *Boundary-Layer Meteorol.* **82**, 219–233.

Irwin, H. P. A. H.: 1979, 'Cross-Spectra of Turbulence Velocities in Isotropic Turbulence', *Boundary-Layer Meteorol.* **16**, 237–243.

Kaimal, J. C. and Gaynor, J. E.: 1991, 'Another Look at Sonic Thermometry', *Boundary-Layer Meteorol.* **56**, 401–410.

Kaimal, J. C., Wyngaard, J. C., Izumi, Y., and Coté, O. R.: 1972, 'Spectral Characteristics of Surface-Layer Turbulence', *Quart. J. Roy. Meteorol. Soc.* **98**, 563–589.

Kristensen, L. and Jensen, N. O.: 1979, 'Lateral Coherence in Isotropic Turbulence and in the Natural Wind', *Boundary-Layer Meteorol.* **17**, 353–373.

Kristensen, L., Mann, J., Oncley, S. P., and Wyngaard, J. C.: 1997, 'How Close is Close Enough when Measuring Scalar Fluxes with Displaced Sensors?', *J. Atmos. Oceanic Tech.* **14**, 814–821.

Lang, A. R. G., McNaughton, K. G., Chen, F., Bradley, E. F., and Ohtaki, E.: 1983, 'Inequality of Eddy Transfer Coefficients for Vertical Transport of Sensible and Latent Heats During Advective Inversions', *Boundary-Layer Meteorol.* **25**, 25–41.

Lee, X., and Black, T. A.: 1994, 'Relating Eddy Correlation Sensible Heat Flux to Horizontal Sensor Separation in the Unstable Atmospheric Surface Layer', *J. Geophys. Res.* **99**(D9), 18,545–18,553.

Leuning, R. and Judd, M. J.: 1996, 'The Relative Merits of Open- and Closed-Path Analysers for Measurement of Eddy Fluxes', *Global Change Biology* **2**, 241–253.

Moore, C. J.: 1986, 'Frequency Response Corrections for Eddy Correlation Systems', *Boundary-Layer Meteorol.* **37**, 17–35.

Neumann, H. H., den Hartog, G., King, K. M., and Chipanshi, A. C.: 1994, 'Carbon Dioxide Fluxes Over a Raised Open Bog at the Kinosheo Lake Tower Site During the Northern Wetlands Study (NOWES)', *J. Geophys. Res.* **99**(D1), 1529–1538.

Oke, T. R.: 1987, *Boundary Layer Climates*, 2nd ed., Methuen Press, London, 435 pp.

Schotanus, P., Nieuwstadt, F. T. M., and de Bruin, H. A. R.: 1983, 'Temperature Measurement with a Sonic Anemometer and its Application to Heat and Moisture Fluxes', *Boundary-Layer Meteorol.* **26**, 81–93.

Wofsy, S. C., Goulden, M. L., Munger, J. W., Fan, S.-M., Bakwin, P. S., Daube, B. C., Bassow, S. L., and Bazzaz, F. A.: 1993, 'Net Exchange of CO_2 in a Mid-Latitude Forest', *Science* **260**, 1314–1317.